

# Exact Bayesian inference for diffusion driven Cox processes

F. B. Gonçalves<sup>a</sup>, K. G. Łatuszyński<sup>b,c</sup>, G. O. Roberts<sup>b</sup>

<sup>a</sup> Departamento de Estatística, Universidade Federal de Minas Gerais, Brazil

<sup>b</sup> Department of Statistics, University of Warwick, UK

<sup>c</sup> Alan Turing Institute

## Abstract

In this paper we present a novel methodology to perform Bayesian inference for Cox processes in which the intensity function is driven by a diffusion process. The novelty lies on the fact that no discretisation error is involved, despite the non-tractability of both the likelihood function and the transition density of the diffusion. The methodology is based on an MCMC algorithm and its exactness is built on retrospective sampling techniques. The efficiency of the methodology is investigated in some simulated examples and its applicability is illustrated in some real data analyses.

*Key Words:* Poisson process, retrospective sampling, infinite dimensionality, MCMC.

## 1 Introduction

Cox processes (Cox, 1955) have been extensively used in a variety of areas to model point process phenomena. Examples can be found in finance - to model credit risk (Chib et al., 2006; Cariboni and Schoutens, 2009), survival analysis (Roberts and Sangalli, 2010), internet traffic (Iversen et al., 2000), insurance (Dassios and Jang, 2003) and Biology (Legg and Chitre, 2012). A Cox process (also sometimes termed doubly stochastic Poisson process) is a Poisson process in which the intensity function (IF) - also known as its rate, evolves stochastically.

We will consider an approach for unidimensional processes which models the evolution of the IF by means of a diffusion process. We call the resulting process a *diffusion driven Cox process* (DDCP). A diffusion process is a continuous time (univariate)

---

<sup>1</sup>Address: Av. Antônio Carlos, 6627 - DEST, ICEX, UFMG - 31270-901, Belo Horizonte, Minas Gerais, Brazil. E-mail: fbgoncalves@est.ufmg.br

Markov process which is defined as the solution of a stochastic differential equation (SDE) of the type:

$$dY_s = \alpha(Y_s; \theta)ds + \sigma(Y_s; \theta)dW_s, \quad Y_0 \sim f_0^*, \quad (1)$$

where  $W_s$  is a Brownian motion. Somewhat more general diffusion processes (eg time inhomogeneous and multivariate) are accessible within the framework we provide. For an accessible introduction to SDE's, see Øksendal (1998).

Suppose  $N := \{N_s; s \in [0, T]\}$  is an one-dimensional inhomogeneous Poisson process (PP) observed in a time interval  $[0, T]$ . In this paper, we consider DDCPs of the type:

$$N \sim PP(\lambda_s), \quad s \in [0, T]; \quad (2)$$

$$\lambda_s = g(X_s, \theta); \quad (3)$$

$$dX_s = \alpha(X_s; \theta)ds + dW_s; \quad (4)$$

$$X_0 \sim f_0(\cdot; \theta). \quad (5)$$

$\lambda := \{\lambda_s; s \in [0, T]\}$  is the IF of the Poisson process and a function  $g$  of a diffusion process  $X := \{X_s; s \in [0, T]\}$ , where  $g(\cdot, \theta) : \mathbb{R} \rightarrow \mathbb{R}$  is non-negative and non-explosive. Also,  $f_0$  is the density of  $X_0$ . The coefficient  $\alpha$  is presumed to satisfy the regularity conditions (locally Lipschitz, with a linear growth bound) that guarantee the existence of a weakly unique, global solution of the SDE.  $\theta$  is a set of parameters. One may choose different parametrisations of the model by manipulating the dependency of  $g$  and  $X$  on  $\theta$ . The parametrisation should be chosen taking into account the interpretation of the model and its impact on the inference methodology - to be discussed further in Section 5.1. Finally, note that we are not restricted to unit diffusion coefficient diffusions. As long as the coefficient  $\sigma$  in (1) is continuously differentiable, we can rewrite a chosen IF  $h(Y)$  as  $g(X)$ , where  $g = h \circ \eta^{-1}$  and  $\eta(y) = \int_{y^*}^y \frac{1}{\sigma(u)} du$ , the Lamperti transform of  $Y$ , for some  $y^*$  in the state space of  $Y$ .

As is common in computational Bayesian methodologies involving intractable likelihoods, carrying out inference under the model in (2)-(5) is closely linked to being able to simulate from the model, itself a particularly challenging problem. As a result of this, existing approaches to this problem (see for example Chib et al. (2006), Cariboni and Schoutens (2009) and Lechnerová et al. (2008)) have resorted to time-discrete approximations, often leading to significant (and often difficult to quantify) bias as well as substantial computational overhead.

The aim of this paper is to propose a methodology which is free of discretisation error to perform simulation and inference for DDCPs as in (2)-(5). The exactness refers to the fact that Monte Carlo error is the only source of approximation. The proposed methodology consists of an MCMC algorithm to sample from the posterior distribution of the unknown components of the model, i.e. parameters and IF. Although the IF is infinite-dimensional, the proposed MCMC is actually based on a finite (albeit varying) dimensional chain. This is due to the retrospective sampling approach adopted, in

which the Markov chain contains the unknown parameters of the model and a random finite-dimensional representation of the IF. This representation is such that the algorithm is tractable and the posterior of the remainder of the IF can be easily recovered from the finite-dimensional representation. This approach is based on previous work on exact inference for diffusions (see Beskos et al., 2006b). Further conditions on functions  $\alpha$  and  $g$  are required but still consider a wide and flexible range of models. In this context, two particular forms for function  $g$  are highlighted, given their good modelling and inference properties. Extensions to consider a different data scheme and to more general models are also discussed. The latter is one based on recent work on exact inference for jump-diffusions (see Gonçalves et al., 2017) that relies on an infinite-dimensional Barker’s MCMC via Bernoulli factories.

Finally, the proposed methodology is investigated in simulated examples and its application is explored with real datasets.

This paper is organised as follows. Section 2 presents the proposed MCMC algorithm to perform exact Bayesian inference for DDCP’s. Simulated and real examples are presented in Sections 3 and 4, respectively. Finally, Section 5 discusses some further topics including model parametrisation, prediction, inference for a different data scheme and extensions of the proposed methodology.

## 2 Bayesian inference for DDCP’s

The posterior distribution of the unknown quantities of the model (IF and parameters) is infinite-dimensional and has intractable posterior density, which makes it unfeasible to devise a straightforward MCMC algorithm to sample from this distribution. Instead, we resort to results related to the exact simulation of diffusions (see Sermaidis et al., 2012) to introduce auxiliary variables that allow us to devise a tractable finite-dimensional MCMC algorithm. Basically, those variables define a finite-dimensional representation of the diffusion which can be sampled exactly from its full conditional distribution and such that, conditional on this representation, the parameters indexing the model are independent of the infinite-dimensional remainder of the diffusion and have a tractable full conditional density. Finally, this approach also allows for exact sampling from the posterior of the infinite-dimensional remainder of the diffusion.

The proposed methodology can be applied to a wide class of models,  $\mathcal{P}_1$ , for which function  $\alpha$  is differentiable and (setting  $A(u) = \int_0^u \alpha(y)dy$  and defining  $\phi_N$  as the Lebesgue density of the standard normal distribution)

- (a)  $\left(g + \frac{\alpha^2 + \alpha'}{2}\right)(u)$  is uniformly bounded below for all  $u \in \mathbb{R}$ ;
- (b)  $\phi_N((u - \mu)/t) \exp\{-A(u)\}f_0(u)$  and  $\phi_N((u - \mu)/t) \exp\{A(u)\}$  are integrable in  $u \in \mathbb{R}$ , for all  $\mu \in \mathbb{R}$ ,  $t > 0$ ;
- (c)  $g(u)$  is bounded by  $\exp\{bu + c\}$ ,  $\forall u \in \mathbb{R}$ , for  $b \geq 0$  and  $c \in \mathbb{R}$ .

Let us start by introducing a random partition  $\tau := (0 = \tau_0 \leq \tau_1 \leq \dots \leq \tau_m \leq \tau_{m+1} = T)$  of the time interval  $[0, T]$ , with  $\Delta_i = \tau_{i+1} - \tau_i$ . Now define  $\{t_j\}_{j=1}^n$  as the events from  $N$  in  $[0, T]$  and, for a fixed  $\tau$ , define  $n_i$  to be the number of observed events in  $[\tau_i, \tau_{i+1}]$ . Let  $(s_{i1}, \dots, s_{in_i})$  be those events and  $\Delta_{ij} = s_{ij} - s_{ij-1}$ , for  $j = 1, \dots, n_i + 1$ ,  $s_{i0} = \tau_i$  and  $s_{in_i+1} = \tau_{i+1}$ . Define the random variables  $\mathcal{L}_i$ ,  $X_\tau$ ,  $\tilde{X}_i$ ,  $\dot{X}_i$  and  $\Xi_i$ , for  $i = 1, \dots, m + 1$ . The random variables  $\mathcal{L}_i$  are called layers and define upper and lower bounds for the path of  $X$  in  $[\tau_i, \tau_{i+1}]$ , details about this are provided in Appendix A2. Furthermore,  $\Xi_i = \{\Xi_{ij}\}$ ,  $j = 1, \dots, n_i + 1$  and  $\Xi_{ij} = \{\Psi_{ij}, \Upsilon_{ij}\}$  is a Poisson process with rate  $r_{ij}(\theta)$  in  $[s_{ij-1}, s_{ij}] \times [0, 1]$  - we shall use the notation  $\psi$  and  $v$  to represent the horizontal and vertical coordinates of the events from  $\Xi_{ij}$ . The rate  $r_{ij}(\theta)$  is a function of  $g$ ,  $\alpha$  and  $\mathcal{L}_i$  and is precisely defined in Appendix A2 - subscript  $j$  makes explicit the dependence of  $r$  on the local behavior of  $\mathcal{L}_i$  in  $[s_{ij-1}, s_{ij}]$ . Finally,  $X_\tau$ ,  $\tilde{X}_i$  and  $\dot{X}_i$  are the diffusion  $X$  at locations  $\tau$ ,  $(s_{i1}, \dots, s_{in_i})$  and  $\Psi_{i\cdot}$ , respectively.

Consider the functions  $\phi$ ,  $\phi_{i,lj}$  and  $\phi_{i,uj}$ , which depend on  $g$ ,  $\alpha$  and  $\mathcal{L}_i$ , as defined in Appendix A2. The posterior density to be targeted by the proposed MCMC algorithm is proportional to the joint density given in the following theorem.

**Theorem 1.** *Let  $\mathbb{L}$  be the Lebesgue measure,  $\mathbb{N}$  be the measure of a unit rate Poisson process on  $[0, T]$ ,  $\tilde{\mathbb{W}}$  be the joint measure of the  $m + 1$  independent Brownian bridges  $BB(\tau_i, X_{\tau_i}; \tau_{i+1}, X_{\tau_{i+1}})$ , for  $i = 0, \dots, m$ , and  $\Xi^+$  be the product measure of  $n + m + 1$  unit rate Poisson processes on  $[s_{ij-1}, s_{ij}] \times [0, 1]$ ,  $\forall i, j$ . Let also  $\pi(\theta)$  be the prior density of the  $p$ -dimensional parameter  $\theta$ . Then, for a fixed value of the partition  $\tau$ , the joint density of  $(N, \mathcal{L}, \tilde{X}, \dot{X}, \Xi, X_\tau, \theta)$  w.r.t. the  $\theta$ -free dominating measure  $\mathbb{L}^{p+1+m+1+\sum_{i=1}^{m+1} n_i} \otimes \mathbb{N} \otimes \tilde{\mathbb{W}} \otimes \Xi^+$  is given by*

$$\begin{aligned} \pi(N, \mathcal{L}, \tilde{X}, \dot{X}, \Xi, X_\tau, \theta) &= \pi(\theta) f_0(X_0; \theta) \exp \{A(X_T; \theta) - A(X_0; \theta)\} \\ &\exp \left\{ \sum_{i=0}^m \sum_{j=1}^{n_i+1} \Delta_{ij} (1 - \phi_{i,uj}(\theta)) \right\} \\ &\prod_{i=0}^m \pi_{\tilde{\mathbb{W}}_i}(\tilde{X}_i) f_{\mathcal{N}}(X_{\tau_{i+1}}; X_{\tau_i}, \Delta_i) \prod_{j=1}^{n_i} g(X_{s_{ij}}; \theta) \\ &\prod_{i=0}^m \prod_{j=1}^{n_i+1} \left[ r_{ij}(\theta)^{\kappa_{ij}} \prod_{k=1}^{\kappa_{ij}} \mathbb{I} \left[ \frac{\phi(\dot{X}_{\psi_{l,i,j}}; \theta) - \phi_{i,lj}(\theta)}{r_{ij}(\theta)} < v_{l,i,j} \right] \right] \end{aligned} \quad (6)$$

**Proof.** See Appendix C.

## 2.1 The MCMC algorithm

In order to sample from the posterior distribution of  $(X, \theta)$ , we propose a Gibbs sampling algorithm that alternates between sampling  $(\mathcal{L}, \tilde{X}, \dot{X}, \Xi, X_0, X_T)$  and  $\theta$  from their respective full conditional distributions - both with density proportional to (6). Note, however, that  $X_\tau$  is not updated. Therefore, in order to make this a valid algorithm to sample from the posterior distribution of the whole diffusion path  $X$  in  $[0, T]$ , we add an extra step to each iteration of the Gibbs sampling to update the random partition  $\tau$ .

This guarantees the irreducibility of the chain and its convergence to the posterior distribution of  $(\mathcal{L}, \tilde{X}, \dot{X}, \Xi, X_\tau, \tau)$ . Finally, simulation from the posterior of the remainder of the diffusion path in  $[0, T]$  is straightforward due to the following corollary.

**Corollary 1.** *The conditional law of  $X$  given  $(X_\tau, \tilde{X}, \dot{X}, \mathcal{L}, N)$  is independent of  $N$  and is given by the joint law of the Brownian bridges between the values  $(X_\tau, \tilde{X}, \dot{X})$ , conditional on layers  $\mathcal{L}$ .*

**Proof.** *See proof of Theorem 1.*

Due to the Markov property,  $(\mathcal{L}, \tilde{X}, \dot{X}, \Xi)$  is conditionally independent among the intervals defined by the partition  $\tau$  and, for each interval  $(\tau_i, \tau_{i+1})$ , for  $i = 1, \dots, m-1$ , it is sampled via rejection sampling. The proposal distribution of the algorithm is a biased Brownian bridge, in the sense that it differs from a Brownian bridge only in the distribution of  $\tilde{X}$ , which has density

$$\pi_{\tilde{\mathbb{W}}_i^*}(\tilde{X}_i) = \frac{1}{c_i(\theta)} \pi_{\tilde{\mathbb{W}}_i}(\tilde{X}_i) \times \prod_{j=1}^{n_i} g(X_{s_{ij}}; \theta), \quad (7)$$

where  $\pi_{\tilde{\mathbb{W}}_i}$  is the density of  $\tilde{X}_i$  under  $BB(\tau_i, X_{\tau_i}; \tau_{i+1}, X_{\tau_{i+1}})$ . Details on how to simulate from the density in (7) are provided in Appendix A1. The acceptance indicator of the proposal is given by:

$$I_i = \mathbb{I} \left[ \exp \left( - \sum_{j=1}^{n_i+1} \Delta_{ij} (\phi_{i,lj}(\theta) - m(\theta)) \right) < u \right] \prod_{j=1}^{n_i+1} \prod_{l=1}^{\kappa_{ij}} \mathbb{I} \left[ \frac{\phi(\dot{X}_{\psi_{l,i,j}}; \theta) - \phi_{i,lj}(\theta)}{r_{ij}(\theta)} < v_{l,i,j} \right], \quad (8)$$

where  $u \sim U(0, 1)$ . The validity of this algorithm is established by Lemma 1 in Appendix A4.

The algorithms to sample  $(\mathcal{L}_i, \tilde{X}_i, \dot{X}_i, \Xi_i)$  for  $i = 0$  and  $i = m$  are slightly different from the algorithm above. Basically, the proposals also include the simulation of  $X_0$  and  $X_T$ , respectively, from the densities

$$\pi_{\mathbb{W}_0^*}(X_0; \theta) \propto \phi_N((X_0 - X_{\tau_1})/\sqrt{\tau_1}) \exp\{-A(X_0; \theta)\} f_0(X_0; \theta), \quad (9)$$

$$\pi_{\mathbb{W}_T^*}(X_T; \theta) \propto \phi_N((X_T - X_{\tau_m})/\sqrt{(T - \tau_m)}) \exp\{A(X_T; \theta)\}. \quad (10)$$

The remainder of the proposal and the acceptance indicator are the same as in the algorithm above. Simulation from (9) and (10) may have to be performed indirectly, for example, via rejection sampling. The flexibility to choose  $f_0$  is useful to assure the integrability of (9). The validity of this algorithm is established by Lemma 1 and Proposition 2 in Appendix A4.

Theorem 1, in particular the fact that the dominating measure in (6) does not depend on  $\theta$ , implies that the full conditional density of  $\theta$  w.r.t. the Lebesgue measure is proportional to (6). This sampling step is further improved by integrating the  $v_{l,i,j}$ 's

out to get

$$\pi(\theta|\cdot) = \pi(\theta)f_0(X_0; \theta) \exp \left\{ A(X_T; \theta) - A(X_0; \theta) - \sum_{i=0}^m \sum_{j=1}^{n_i+1} \Delta_{ij} \phi_{i,u_j}(\theta) \right\} \\ \prod_{i=0}^m \left[ \prod_{j=1}^{n_i} g(X_{s_{ij}}; \theta) \right] \left[ \prod_{j=1}^{n_i+1} r_{ij}(\theta)^{\kappa_{ij}} \prod_{k=1}^{\kappa_{ij}} \left( 1 - \frac{\phi(\dot{X}_{\psi_{l,i,j}}; \theta) - \phi_{i,l_j}(\theta)}{r_{ij}(\theta)} \right) \right]. \quad (11)$$

A Metropolis step will typically be required to sample from this distribution.

Finally, one appealing proposal on how to update the partition  $\tau$  is presented in Appendix A3.

## 2.2 Efficiency of the algorithm

Note that we are free to choose how to update the partition  $\tau$  in the Gibbs sampler. Naturally, this choice has great impact on the efficiency of the algorithm. In one direction, the smaller number of subintervals is, the lower is the autocorrelation of the chain, leading to faster convergence. On the other hand, the acceptance probability of the rejection sampling algorithm that samples  $(\mathcal{L}_i, \tilde{X}_i, \dot{X}_i, \Xi_i)$  decreases (exponentially) as the length of the time interval increases. A reasonable empirical strategy is to choose the minimum number of subintervals for which the computational cost is tolerable. Naturally, this depends heavily on functions  $\alpha$  and  $g$ .

The computational cost to update  $(\mathcal{L}_i, \tilde{X}_i, \dot{X}_i, \Xi_i)$  may substantially vary among the different sub-intervals defined by the partition  $\tau$ . This is related to the variation of function  $\phi$  which, in turn, is related to the information in the data. Typically, time regions with a higher concentration of events will lead to higher variations in the IF and, therefore, higher variations in function  $\phi$ , resulting in a small acceptance probability. This behavior is usually easy to be identified in each example. A reasonable strategy to mitigate the problem is to adopt a partition  $\tau$  with different sized subintervals. As long as this is predefined for the MCMC, the algorithm is still valid. In particular, one may fix the number of subintervals in sequence that should have the same size until a different size is considered.

The number of time points defining the partition  $\tau$  -  $m$ , will be typically large and, therefore, induce a high autocorrelation for the diffusion  $X$ . This will, in turn, lead to a high autocorrelation of the parameter vector  $\theta$ . A simple strategy to alleviate this problem is to perform multiple updates of  $\tau$  and  $(\mathcal{L}, \tilde{X}, \dot{X}, \Xi, X_0, X_T)$  for each update of  $\theta$ . Furthermore, Monte Carlo estimation should be performed using a thinned sample of  $X$ .

Some important parametrisation issues related to the efficiency of the MCMC algorithm are discussed in Section 5.1.

### 3 Examples

We present some simulated examples to investigate the modelling and inference properties of the proposed methodology. We consider two examples for the link function  $g$  which have great modelling and inference appeal. The first example is the exponential function, widely used through the well-known Log-Gaussian Cox process (Møller et al., 1998; Diggle, 2014). The second one is the standard normal cdf  $\Phi$ , also used for Gaussian process driven Cox processes (Gonçalves and Gamerman, 2018). Those functions feature the nice property of going from  $\mathbb{R}$  to  $\mathbb{R}^+$  and  $[0, 1]$ , respectively. We combine those functions with three diffusion models, each one solving one of the following SDE's:

$$\begin{aligned} dX_s &= -\rho X ds + dW_s \quad (\text{Ornstein-Uhlenbeck - OU}); \\ dX_s &= -\rho X_s(\sigma^2 X_s^2 - \mu) ds + dW_s. \quad (\text{transformed double well potential - DW}); \\ dX_s &= -\frac{X_s}{1 + X_s^2} ds + dW_s \quad (\text{Cauchy}). \end{aligned}$$

The OU-process is a stationary Gauss-Markov process and the Cauchy process has a Cauchy invariant distribution which basically allows for longer term excursions away from 0 than a Gaussian process. The double well process stochastically alternates visits between two regions around locally reversible values. In Appendix B, we present some simulated trajectories and Monte Carlo estimates for some models that combine the two link functions above with the OU and double well diffusions. The algorithm to simulate from the model is also presented there.

Now, we present three simulated examples, in which the first two aim at analysing how well the IF function and model parameters are estimated and the third one explores model flexibility. In the first two, data is simulated in the interval  $[0, 400]$  and the proposed MCMC algorithm is run to estimate the intensity function and parameters indexing the model. Given the low information that the data contains about the volatility parameter  $\sigma$  and the feasibility to fix it in a reasonable value (see discussion in Section 5.1), this parameter is fixed in its real value. The chains run for 51000 iterations with a burn-in of 11000, with the parameter vector being updated from iteration 1020 at every 20 iterations of the Gibbs sampler and performing (for the exp-OU example) 40 consecutive updates per time. A lag of 20 iterations is considered to obtain the posterior sample of the diffusion path. A noncentred parametrisation (see Section 5.1) is adopted for the Poisson processes  $\Xi_{ij}$  in the cdf-DW example. These are all strategies to optimise the chain's convergence speed. All the estimated parameters in each model are jointly sampled via Metropolis Hastings with a properly tuned Gaussian random walk proposal. The algorithms are implemented in Ox (Doornik, 2007) and run in a 3.50-GHz Intel i7 processor with 16GB RAM.

We fit the exp-OU -  $g(X_s) = \exp(\mu + \sigma X_s)$ , and the cdf-DW -  $g(X_s) = \delta \Phi(\sigma X_s)$ , models to the respective datasets presented in Figure 6. They have 499 and 645 events, respectively. We estimate parameters  $\mu$  and  $\rho$  for the former and  $\delta$  for the latter. The remaining parameters are fixed at their real value. Note that, in the cdf-DW model, there is an intrinsic identifiability issue if parameter  $\delta$  is unknown. This is basically

because an increase in the value of  $\delta$  can be compensated by a change in the parameters of the DW diffusion in order to reduce the amplitude of its variation and vice-versa. Furthermore, the form of the IF may ravel the identification of the diffusion path as it goes away from 0 which, in turn, may compromise the joint identification of parameters  $\mu$  and  $\rho$ . A reasonable solution is to fix the diffusion parameters according to the time scale of the problem - the example presented here can be used as a reference for the DW process.

We adopt  $f_0(u) \propto \exp(-\rho\sigma^2x^4/4)$  so that  $\pi_{\mathbb{W}_0^*}(u) \propto \phi_N((u-\mu)/\sigma) \exp\{-A(u)\} f_0(u)$  is integrable for the cdf-DW example. Improper constant priors are adopted for all parameters and the results are presented in Figure 1 and Table 1. Trace plots and autocorrelation plots of the parameters are shown in Figure 5 of Appendix D.

	$\delta$			$\mu$			$\rho$			$\sigma$
	real	mean	sd	real	mean	sd	real	mean	sd	real
exp-OU	-	-	-	0	0.134	0.142	0.05	0.097	0.031	0.2
cdf-DW	3	3.192	0.399	1	-	-	0.1	-	-	0.2

Table 1: Posterior statistics of the estimated parameters for both simulated examples. Parameters without an estimate were fixed at their real values.

The general class of Cox process models proposed in this paper offers significant contribution, in terms of model flexibility, when compared to the class of models found in the existing literature, in particular log-Gaussian Cox processes. In order to illustrate this, we compare a heavy tailed DDCP - the exp-Cauchy model, to the exp-OU model, which is a log-Gaussian Cox process. The exp-Cauchy model considers the intensity function to be the exponential of the Cauchy diffusion -  $g(X_s) = \rho \exp(\sigma X_s)$ . We generate data from the exp-Cauchy model in  $[0, 1000]$  for  $\rho = 0.2$  and  $\sigma = 0.4$ . The dataset contains 353 points. We fit both the exp-Cauchy and the exp-OU model and predict two functionals of the intensity function in  $[1000, 2000]$ ,  $I_\lambda = E[\int_{1000}^{2000} \lambda_s ds]$  and  $p_\lambda = E[p_4(\lambda_s)]$ , where  $p_4(\lambda_s)$  is the proportion of times the intensity function goes above 4 at time points multiple of 0.1 in  $[1000, 2000]$ . We also compare the predicted IF with some replication of data in  $[1000, 2000]$ . That is done by computing MC estimates of:

$$E_f = E \left[ \frac{1}{50} \sum_{i=1}^{50} f(|I_{\lambda,i} - N_i|) \right], \quad (12)$$

where  $I_{\lambda,i}$  is the predictive integrated IF in  $[1000 + 50(i - 1), 1000 + 50i]$  and  $N_i$  is the number of events in the same time interval from the simulated data. We consider two options for function  $f$ ,  $f_1(\Delta) = 2(F_{t,1}(\Delta^2/1000) - 0.5)$ , where  $F_{t,1}$  is the cdf of a student-t distribution with 1 d.f., and  $f_2(\Delta) = \Delta/(I_{\lambda,i} - N_i)$ , where  $\Delta = |I_{\lambda,i} - N_i|$ . These statistics are computed for 1000 replications of data in  $[1000, 2000]$  and we analyse the distribution of this sample.

Figure 2 shows the real and estimated IF under the two models. Figure 3 and Table 2 show the results for the predictive distribution. Although the estimation of the IF is similarly efficient under both models, their predictive power is substantially different.



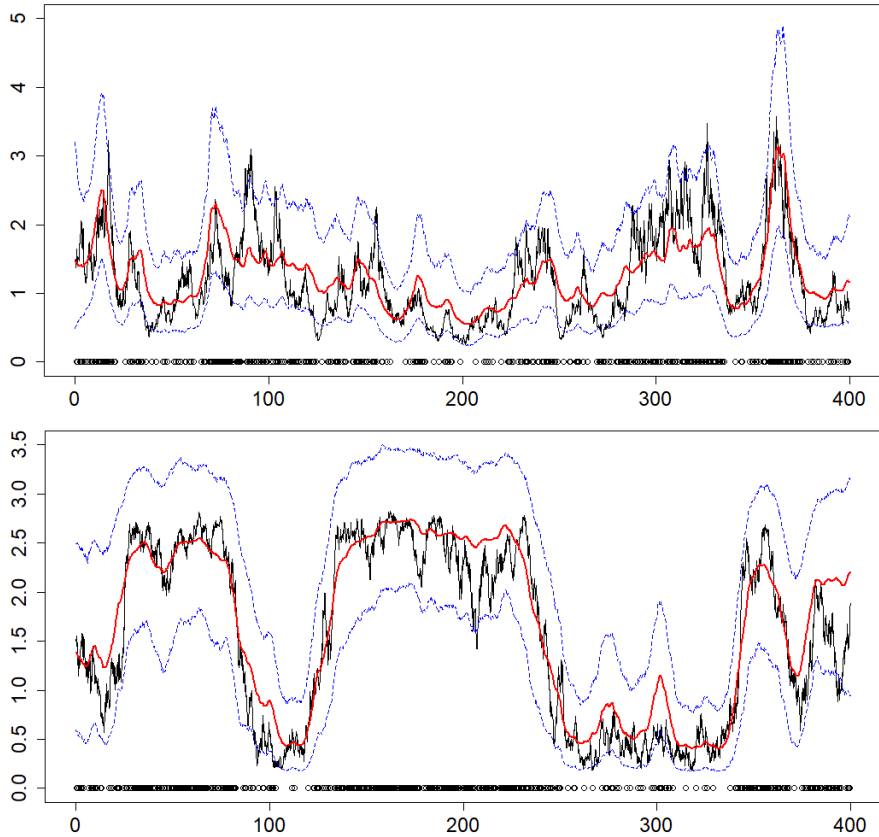


Figure 1: Real (black line) and estimated intensity function - posterior mean and point-wise 95% credibility interval, for the exp-OU (top) and cdf-DW (bottom) examples. The black circles represent the data.

The model misspecification does not have great impact on the IF estimation but leads to highly biased predictions.

		$I_\lambda$										
		min	1%	5%	10%	25%	50%	75%	90%	95%	99%	max
exp-OU		594.1	1548.3	2487.4	3153.2	4864.4	8666.7	17847.2	40055.6	74540.4	$3.1 \times 10^5$	$9.8 \times 10^7$
exp-Cauchy		2.7	276.5	425.7	552.9	1062.5	4333.1	72307.5	$6.1 \times 10^6$	$3.3 \times 10^8$	$6.1 \times 10^{13}$	$9.5 \times 10^{38}$
		$p_\lambda$										
		min	1%	5%	10%	25%	50%	75%	90%	95%	99%	max
exp-OU		0	0	0	0	0	0	0	0	0	0	0
exp-Cauchy		0	0.0028	0.011	0.019	0.039	0.065	0.117	0.180	0.242	0.437	0.975

Table 2: Comparison of predictive estimates under the exp-OU and exp-Cauchy models.

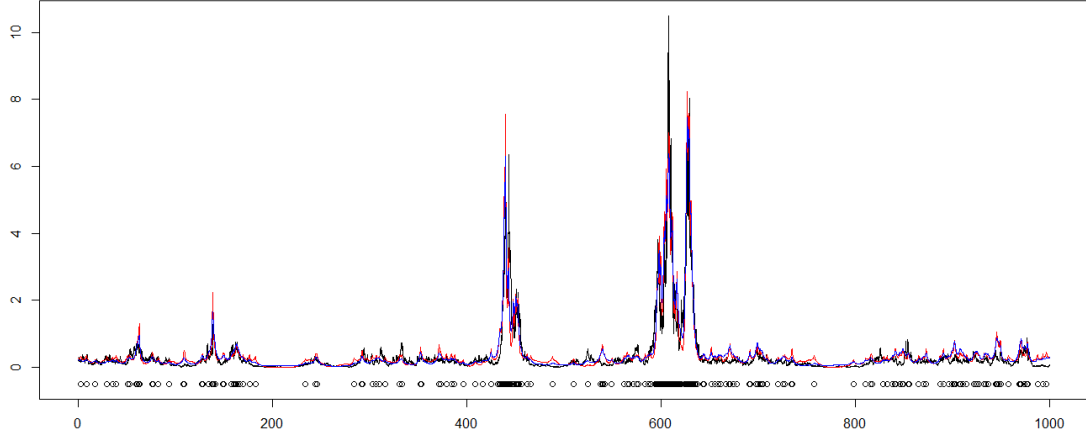


Figure 2: Real (black line) and estimated intensity function - under the exp-OU (blue) and exp-Cauchy (red) models. The black circles represent the data.

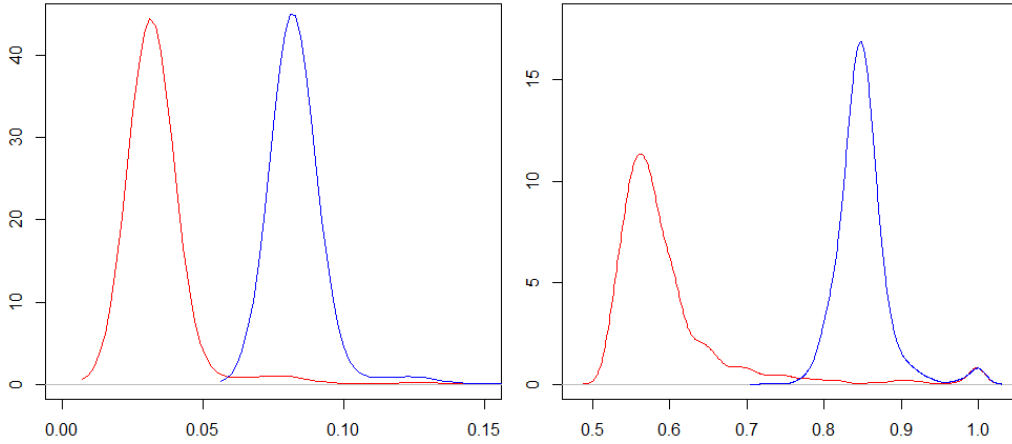


Figure 3: Distribution of the MC estimates  $E_{f_1}$  (left) and  $E_{f_2}$  (right) under the Exp-Cauchy (red) and Exp-OU (blue) models, for the 1000 data replications. The sample for  $f_1$  presents values up to 1, but with negligible density above 0.15. The sample for  $f_1$  has mean and s.d. 0.053 and 0.111 for the Cauchy model and 0.102 and 0.104 for the OU model. The sample for  $f_2$  has mean and s.d. 0.600 and 0.086 for the Cauchy model and 0.850 and 0.034 for the OU model.

## 4 Applications

We apply the proposed methodology to three real datasets. The first one is the classic coal mine disaster data of Jarrett (1979), consisting of the dates of 191 coal mine explosions that killed ten or more men in Britain between March 15th, 1875 and March 22nd, 1962. We consider year as the time unit and the cdf-DW model. Parameter  $\delta$  is estimated and we fix  $\mu = 1$ ,  $\rho = 0.1$  and  $\sigma = 0.2$ . The second dataset regards the SP500 index from January 3rd, 2000 to December 31st, 2013 - 3521 days, with data consisting of the days in which a variation of more than 20 points occurred - 489 days in total

(13,89%). The exp-OU model is considered with one time unit corresponding to ten days and for fixed  $\sigma = 0.2$ . Finally, the third dataset considers earthquake occurrences in Japan (rectangular region containing all the main islands from Kyushu to Hokkaido) from Jan 1st 2014 to 29th Oct 2018, with magnitude 4,5+. The exp-Cauchy model is considered with day as the time unit. Parameters  $\rho$  and  $\sigma$  are constrained to be smaller than 1, to avoid computational cost problems. Results are presented in Figures 4 and 5 and Table 3.

	$\delta$		$\mu$		$\rho$		$\sigma$	
	mean	sd	mean	sd	mean	sd	mean	sd
Coal mine (cdf-DW)	5.105	1.094	-	-	-	-	-	-
SP500 (exp-OU)	-	-	-0.517	0.866	0.013	0.0083	-	-
Japan_EQ (exp-Cauchy)	-	-	-	-	0.801	0.119	0.782	0.132

Table 3: Posterior statistics of the estimated parameters for the three applications.

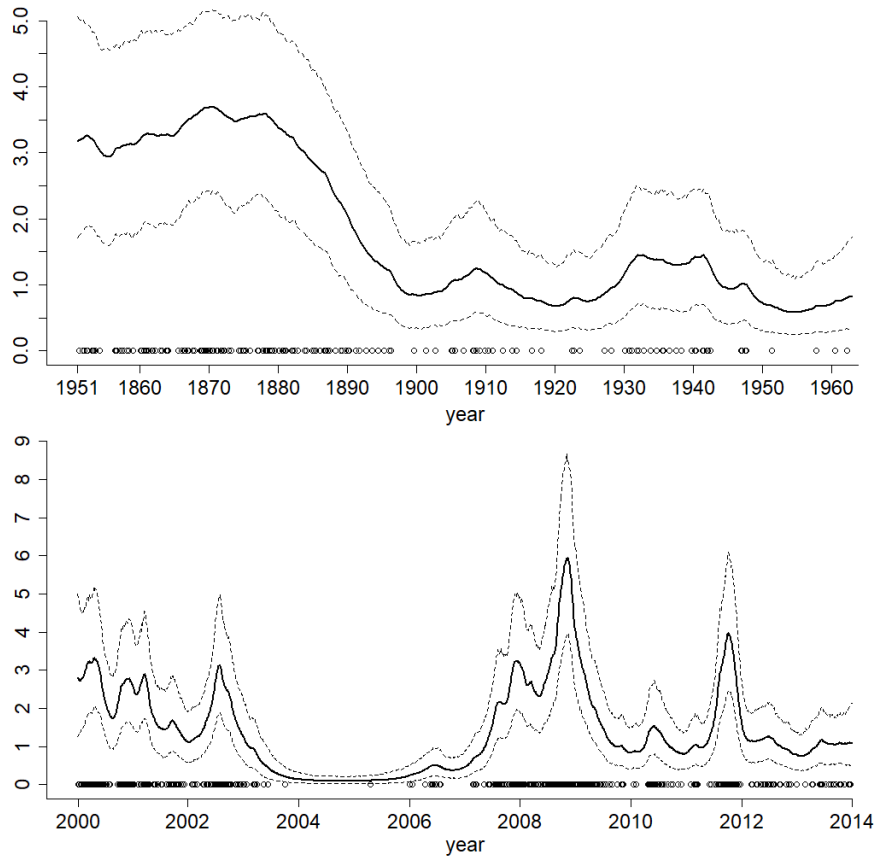


Figure 4: Estimated intensity function - posterior mean and pointwise 95% credibility interval, for the coal mine - cdf-DW (top), and SP500 - exp-OU (bottom), examples.

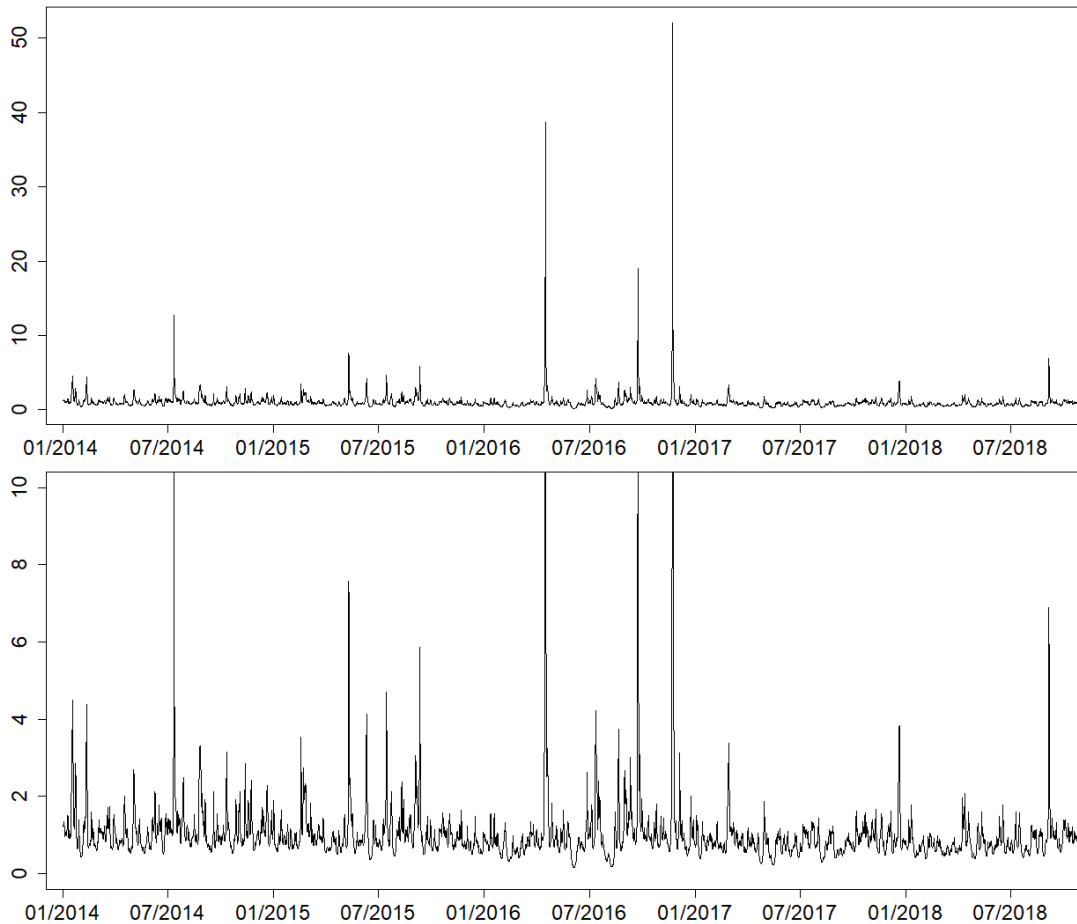


Figure 5: Estimated intensity function - posterior mean, for the Japan earthquake example. The plot on the bottom zooms the estimate in  $[0, 10]$ .

## 5 Further topics

### 5.1 A note on parametrisation

The general DDCP model defined in (2)-(5) will sometimes admit different parametrisations. Typically, the parametrisation of a model has great impact on the efficiency (convergence properties) of the MCMC algorithm devised to perform inference. We define  $\eta_1$  as the set of parameters indexing function  $g$  and  $\eta_2$  as the set indexing functions  $\alpha$  and  $f_0$ .

We consider the parametrisation issue when the same model may be defined with some parameter(s) being either in  $\eta_1$  or  $\eta_2$ , referred to as noncentred and centred parametrisations, respectively. This problem is deeply investigated in Papaspiliopoulos et al. (2007), in a general Gibbs sampling context, who argue that the noncentred parametrisation performs better when  $X$  (the missing data), under the centred parametrisation, is relatively (to the parameter(s) in question) weakly identified by the data. This implies that  $X$ , under the noncentred parametrisation, and the parameter(s) in question

are not highly correlated a posteriori, which contributes to the efficiency of the Gibbs sampler.

In the context of DDCP, the diffusion  $X$ , under the centred parametrisation, is strongly identified by the data, relatively to the parameters indexing the diffusion, because the data is highly informative about the intensity function. For that reason, the centred parametrisation should always be preferred (see Figure 8 in Appendix D).

It is also important to address the fact that the Poisson process data is, typically, not very informative about the parameters indexing the diffusion. This is basically due to the composition of the Poisson process variance given the IF and the diffusion variance given its parameters. The same phenomenon is observed, for example, for Gaussian process driven Cox processes (see Gonçalves and Gamerman, 2018).

Finally, note that some parameters may eventually appear in both  $\eta_1$  and  $\eta_2$ , that is the case if the model is defined based on a diffusion  $Y$  with a diffusion coefficient depending on unknown parameters. Estimation of those parameters should be avoided and, given that the diffusion coefficient determines the instant variance of the diffusion, it is reasonable to assume that the data will contain even less information about those parameters when compared to parameters in the drift. For that reason, fixing the parameters in the diffusion coefficient, based on the scale of the problem, should be feasible and lead to good results. If, however, estimation of those parameter is indispensable, the MCMC algorithm should be devised in terms of  $Y = \eta^{-1}(X)$  (the inverse of the Lamperti transform) instead of  $X$ , so that the centred parametrisation can be considered also for parameters in the diffusion coefficient. In practice, the new algorithm will only differ from that in Section 2 in terms of the full conditional distribution of  $\theta$ . Defining  $X_i(\theta) = \eta(Y_{\tau_i}; \theta)$ ,  $X_{ij}(\theta) = \eta(Y_{s_{ij}}; \theta)$  and  $X_{t_j}(\theta) = \eta(Y_{t_j}; \theta)$ , this distribution is given by

**Theorem 2.**

$$\begin{aligned} \pi(\theta|\cdot) = & \pi(\theta) f_0^*(Y_0; \theta) \exp \left\{ A(X_T(\theta); \theta) - A(X_0(\theta); \theta) - \sum_{i=0}^m \sum_{j=1}^{n_i+1} \Delta_{ij} \phi_{i,u_j}(\theta) \right\} \\ & \prod_{i=0}^m p_{i|\bar{w}_i}(\tilde{X}_i(\theta); X_{\tau_i}(\theta), X_{\tau_{i+1}}(\theta)) f_{\mathcal{N}}(X_{\tau_{i+1}}(\theta); X_{\tau_i}(\theta), \Delta_i(\theta)) \eta'(Y_{\tau_{i+1}}; \theta) \prod_{j=1}^{n_i} \eta'(Y_{s_{ij}}; \theta) \\ & \prod_{i=0}^m \left[ \prod_{j=1}^{n_i} g(X_{ij}(\theta); \theta) \right] \left[ \prod_{j=1}^{n_i+1} r_{ij}(\theta)^{\kappa_{ij}} \prod_{k=1}^{\kappa_{ij}} \left( 1 - \frac{\phi(\varphi(\omega_{\psi_{k,i,j}}; x_{ij-1}(\theta), x_{ij}(\theta)); \theta) - \phi_{i,l_j}(\theta))}{r_{ij}(\theta)} \right) \right]. \end{aligned}$$

where  $\omega$  are the standard Brownian bridges from the diffusion simulation and  $\varphi(\omega_{\psi_{k,i,j}}; x_{ij-1}(\theta), x_{ij}(\theta))$  is the linear transformation that recovers the bridges of  $X$  from the standard BB's.

**Proof.** See Appendix C.

Another possible reparametrisation regards the Poisson processes  $\Xi_i$ . Basically, some models may induce a high correlation between the parameters indexing the diffusion and the PP's  $\Xi_i$ . Sermaidis et al. (2012) proposes a noncentred parametrisation to

reduce that dependence that, instead of simulating a Poisson process with rate  $r_{ij}(\theta)$  on  $[0, t] \times [0, 1]$ , simulates a Poisson process with rate 1 on  $[0, t] \times [0, \infty)$ . This strategy works because we only need to unveil the points for which the second coordinate falls below  $r_{ij}(\theta)$ . This leads to the following full conditional distribution for  $\theta$ :

**Theorem 3.**

$$\begin{aligned} \pi(\theta|\cdot) &\propto \prod_{j=1}^n g(\eta^{-1}(X_{t_j}; \theta)) f_0(X_0; \theta) \pi(\theta) \\ &\exp \left\{ A(X_T; \theta) - A(X_0; \theta) - \sum_{i=0}^m \sum_{j=1}^{n_i+1} \Delta_{ij} \phi_{i,l_j}(\theta) \right\} \\ &\prod_{i=0}^m \prod_{j=1}^{n_i+1} \left[ \prod_{k=1}^{\infty} \left( 1 - \mathbb{I}(v_{k,i,j} < r_{ij}(\theta)) \frac{\phi(\dot{X}_{\psi_{k,i,j}}; \theta) - \phi_{i,l_j}(\theta)}{r_{ij}(\theta)} \right) \right]. \end{aligned} \quad (13)$$

**Proof.** *Combines the proof of Theorem 1 and that of Theorem 3 from Sermaidis et al. (2012).*

The practical computational difference compared to the original algorithm is that, when proposing a move from  $\theta$  to  $\theta^*$ , one needs to simulate potential extra PP points if  $r_{ij}(\theta^*) > r_{ij}(\theta)$  (see Sermaidis et al., 2012, Section 4.1). The double well potential process is a typical example in which the noncentred parametrisation leads to significant improvement (see Figure 9 in Appendix D).

## 5.2 Prediction

Prediction about future behavior is generally of interest when fitting unidimensional Cox processes. Under the Bayesian Paradigm, that is naturally achieved through the predictive distribution, i.e. the posterior distribution of some function of the process in some unobserved time interval.

It is straightforward to obtain a sample from the predictive distribution in an MCMC context, as it is considered in this paper. Suppose that we want to predict some function  $h(N^*, X^*)$  of the Cox process and the diffusion  $X$  in some unobserved time interval, given data  $N$ . The predictive distribution of  $h(N^*, X^*)$  satisfies:

$$\pi(h(N^*, X^*)|N) = \int \pi(h(N^*, X^*)|X, \theta) \pi(X, \theta|N) dX d\theta. \quad (14)$$

This means that a sample from the predictive distribution  $\pi(h(N^*, X^*)|N)$  can be obtained by simulating one observation from  $\pi(h(N^*, X^*)|X^{(j)}, \theta^{(j)})$ , for each  $(X^{(j)}, \theta^{(j)})$  in the posterior sample output in the MCMC algorithm. Naturally, simulation from  $\pi(h(N^*, X^*)|X, \theta)$  should be possible.

Consider for example  $h(N^*, X^*) = N_{T+t^*} - N_T$ , for some  $t^* > 0$ , i.e. the number of events in the interval of length  $t^*$  following the observed interval. Simulation from  $\pi(h(N^*, X^*)|N)$  is performed as follows:

**Simulation from the predictive distribution**

1. initiate  $j = 1$ ;
2. simulate  $X^{*(j)} := \{X_t; T \leq t^* \leq T + t^*\}$ , given  $X_T^{*(j)}$  and  $\theta^{(j)}$ , and keep the bounds for  $X^*$ ;
3. obtain an upper bound  $\lambda^*$  for  $\lambda_s$  in  $[T, T + t^*]$  using the bounds for  $X^*$ ;
4. simulate a Poisson process of rate  $\lambda^*$  on  $[0, t^*]$ ;
5. simulate  $X^*$  at the times of the  $PP(\lambda^*)$ ;
6. keep each of the events  $t_i$  with probability  $R(t_i) = \frac{g(X_{t_i}^{*(j)}, \theta^{(j)})}{\lambda^*}$ .
7. store  $N_{T+t^*}^{(j)} - N_T$ , make  $j = j+1$  and go to 2 until the whole MCMC sample is used.

Steps 2 and 5 are performed via the EA algorithm (Beskos et al., 2008) that performs exactly simulation of a class of diffusion processes.

It is also feasible to devise unbiased Monte Carlo estimators for expectations of intractable functions  $h$  under the predictive distribution. For example, suppose that we want to estimate  $I = E_{(X^*, \theta|N)} \left[ \int_T^{T+t^*} g(X_s, \theta) ds \right]$ . Unbiased estimation is achieved by defining a r.v.  $U$  with uniform distribution in  $(T, T + t^*)$  and noting that

$$I = t^* E_{(U, X_0, \theta|N)} [g(X_U, \theta)]. \quad (15)$$

This means that an unbiased estimator of  $I$  is given by:

$$\hat{I} = t^* \frac{1}{J} \sum_{j=1}^J g(X_{U^{(j)}}^{(j)}, \theta^{(j)}), \quad (16)$$

which can be computed by simulating  $J$  iid samples of  $U$  and  $X_U$ , the latter from its predictive distribution.

### 5.3 Inference for a different data scheme

Suppose that instead of observing the complete Poisson process  $N$ , we only observe the number of points in a collection of intervals defining a partition of  $[0, T]$ . This is a common feature in real datasets in which data are aggregated in small time intervals (w.r.t. the total observed time interval), like daily counting data for processes observed over months/years.

Define  $\Gamma := (0 = \gamma_0, \gamma_1, \dots, \gamma_r = T)$  to be the  $r+1$  time points defining the partition in which the aggregated data is observed and  $\dot{n} := (\dot{n}_1, \dots, \dot{n}_r)$  to be the number of points in each of the intervals from the partition. Poisson process properties imply that the  $\dot{n}_j$ 's are all conditionally independent (given the intensity function) and

$$\dot{n}_j \sim \text{Poisson} \left( \int_{\gamma_{j-1}}^{\gamma_j} g(X_s; \theta) ds \right). \quad (17)$$

which leads to the following likelihood function:

$$L(X, \theta) \propto \exp \left\{ - \int_0^T g(X_s; \theta) ds \right\} \prod_{j=1}^r \left( \int_{\gamma_{j-1}}^{\gamma_j} g(X_s; \theta) ds \right)^{\dot{n}_j}. \quad (18)$$

Inference for this data scheme can be carried out for models in the  $\mathcal{P}_1$  class that, additionally, have a bounded intensity function conditional on the parameters, for example, the cdf-\* models. Suppose that  $M(\theta)$  is an upper bound for  $g(u; \theta)$ ,  $u \in \mathcal{X}$ . We consider a Gibbs sampling algorithm analogous to the one proposed in Section 2. The partition  $\tau$  of  $[0, T]$  needs to be discretely distributed over  $\Gamma$  such that each interval  $(\tau_{l-1}, \tau_l)$  needs to contain at least two of the subintervals defined by  $\Gamma$  so that  $\tau$  can be updated to assure irreducibility of the chain.

The diffusion bridges are sampled in each subinterval  $(\tau_i, \tau_{i+1})$  via rejection sampling by proposing from a Brownian bridge and accepting with probability:

$$\alpha_1 = \exp \left\{ - \int_{\tau_i}^{\tau_{i+1}} \phi(X_s; \theta) - m(\theta) ds \right\} \prod_{j \in \tau_{i,i+1}} \left( \frac{\int_{\gamma_{j-1}}^{\gamma_j} g(X_s; \theta) ds}{(\gamma_j - \gamma_{j-1}) M(\theta)} \right)^{\dot{n}_j}, \quad (19)$$

for  $\phi$  and  $m(\theta)$  as in Appendix A2 and  $\tau_{i,i+1}$  representing the set of observed intervals that define  $(\tau_i, \tau_{i+1})$ . The acceptance probability in (19) is evaluated by simulating a Poisson process for the exponential term and by computing an unbiased (and a.s. in  $(0, 1)$ ) estimator for the product term.

Define  $r_i$ ,  $\phi_{i,l}$  and  $\phi_{i,u}$  as in Appendix A2, by making  $n_i = 0$ , and consider the indicator function

$$I_i = \mathbb{I} \left[ \exp(-\Delta_i(\phi_{i,l}(\theta) - m(\theta))) < u \right] \prod_{l=1}^{\kappa_i} \mathbb{I} \left[ \frac{\phi(\dot{X}_{\psi_{l,i}}; \theta) - \phi_{i,l}(\theta)}{r_i(\theta)} < v_{l,i} \right], \quad (20)$$

where  $u \sim U(0, 1)$ .

Furthermore, an unbiased estimator of the product term in (19) is given by

$$\prod_{j \in \tau_{i,i+1}} \prod_{l=1}^{\dot{n}_j} \frac{g(X_{U_{j,l}}; \theta)}{M(\theta)}, \quad (21)$$

where  $U_j = (U_{j,1}, \dots, U_{j,\dot{n}_j})$  and the  $U_{j,l}$ 's are iid  $U(\gamma_{j-1}, \gamma_j)$ . Finally, the initial and ending intervals are sampled by proposing from a biased Brownian motion which bias the extreme points with terms  $\exp\{-A(X_0; \theta)\}$  and  $\exp\{A(X_T; \theta)\}$ , respectively.

The full conditional density of the parameter vector  $\theta$  is derived analogously to Theorem 1 and is given by:

$$\begin{aligned} \pi(\theta|\cdot) &\propto M(\theta)^{\sum_{j=1}^r \dot{n}_j} f_0(X_0; \theta) \pi(\theta) \\ &\exp \left\{ A(X_T; \theta) - A(X_0; \theta) - \sum_{i=0}^m \Delta_i \phi_{i,u}(\theta) \right\} \\ &\prod_{i=0}^m \left[ (r_i(\theta))^{\kappa_i} \prod_{l=1}^{\kappa_i} \left( 1 - \frac{\phi(\dot{X}_{\psi_{l,i}}; \theta) - \phi_{i,l}(\theta)}{r_i(\theta)} \right) \right]. \end{aligned} \quad (22)$$



## 5.4 Extensions

The methodology proposed in this paper is restricted to the class  $\mathcal{P}_1$  defined in Section 2. Although this is a rich class, one may wonder whether the methodology could be extended to a wider class of models. In fact, we can combine the theory in this paper with ideas from Gonçalves et al. (2017) to devise an exact methodology for a wider class of models that only requires the drift  $\alpha$  to be differentiable.

Gonçalves et al. (2017) devise a general MCMC algorithm to perform exact inference for discretely observed (jump-)diffusion processes. The algorithm consists of a Gibbs sampling that alternates between updating parameters and missing paths between observations. Each of those two blocks are updated via Barker's steps in which the unknown acceptance probabilities are evaluated using a Bernoulli Factory (see Łatuszyński et al., 2011) called the 2-coin algorithm. This could be adapted to DDCP's by adding the Poisson process likelihood (33) to the expression of the acceptance probability in each step of the Gibbs sampling.

Finally, this extended methodology could also be applied to the data scheme described in Section 5.3 for any diffusion with differentiable drift  $\alpha$ .

## 6 Conclusions

This paper proposes the first exact methodology to perform inference in a class of diffusion driven Cox processes. The methodology is exact in the sense that no discretisation-based approximation is used and MCMC error is the only source of inaccuracy. The proposed MCMC algorithm is a Gibbs Sampling that alternates between updating the diffusion path and the parameters indexing the model.

The exactness feature of the algorithm lies on the key fact that the global acceptance probability of the rejection sampling algorithm that samples from the full conditional distribution of the diffusion (bridges) has an intractable term which also appears in the joint density of the data and the diffusion at a finite collection of time points.

A number of issues related to model flexibility and the efficiency of the proposed methodology is discussed and illustrated in simulated examples. Results show very good recovery of the intensity function and the Cauchy diffusion example illustrates the model flexibility when compared to the most popular models in the literature. Also, three real data examples are present, concerning coal mine accidents, the SP500 index and earthquakes in Japan.

Further discussions are presented regarding model parametrisation, prediction and inference for the case where the data is aggregated. The centred parametrisation is argued and illustrated to have a better performance. Prediction is straightforwardly performed in an extra sampling step that uses the MCMC output to sample from the desired predictive distribution. Finally, an extension of the proposed methodology for a wider class of models is discussed with the use of an infinite-dimensional Barker's MCMC algorithm.

## References

- Beskos, A., Papaspiliopoulos, O., and Roberts, G. O. (2006a). Retrospective exact simulation of diffusion sample paths with applications. *Bernoulli*, 12(6):1077–1098.
- Beskos, A., Papaspiliopoulos, O., and Roberts, G. O. (2008). A new factorisation of diffusion measure and sample path reconstruction. *Methodology and Computing in Applied Probability*, 10(1):85–104.
- Beskos, A., Papaspiliopoulos, O., Roberts, G. O., and Fearnhead, P. (2006b). Exact and computationally efficient likelihood-based inference for discretely observed diffusion processes (with discussion). *Journal of the Royal Statistical Society, Series B*, 68(3):333–382.
- Cariboni, J. and Schoutens, W. (2009). Jumps in intensity models: investigating the performance of Ornstein-Uhlenbeck processes in credit risk modeling. *Metrika*, 69:173–198.
- Chib, S., Pitt, M. K., and Shephard, N. (2006). Likelihood based inference for diffusion driven state space models. *Working paper*.
- Cox, D. R. (1955). Some statistical methods connected with series of events. *Journal of the Royal Statistical Society, Series B*, 17:129–164.
- Dassios, A. and Jang, J. (2003). Pricing of catastrophe reinsurance and derivatives using the cox process with shot noise intensity. *Finance and stochastics*, 7:73–95.
- Diggle, P. J. (2014). *Statistical Analysis of Spatial and Spatio-Temporal Point Patterns*. Chapman & Hall, London, 3rd edition.
- Doornik, J. A. (2007). *Object-Oriented Matrix Programming Using Ox*. Timberlake Consultants Press and Oxford, London, 3rd edition.
- Gonçalves, F. B. and Gamerman, D. (2018). Exact Bayesian inference in spatio-temporal Cox processes driven by multivariate Gaussian processes. *Journal of the Royal Statistical Society - Series B*, 80(157-175).
- Gonçalves, F. B., Roberts, G. O., and Łatuszynski, K. G. (2017). Exact Monte Carlo likelihood-based inference for jump-diffusion processes. [*arXiv:1707.00332*].
- Iversen, V. B., Glenstrup, A. J., and Rasmussen, J. (2000). Internet dial-up traffic modelling. *Fifteenth Nordic Teletraffic Seminar*.
- Jarrett, R. G. (1979). A note on the intervals between coal-mining disasters. *Biometrika*, 66:191–193.
- Łatuszyński, K., Kosmidis, I., Papaspiliopoulos, O., and Roberts, G. (2011). Simulating events of unknown probabilities via reverse time martingales. *Random Structures & Algorithms*, 38(4):441–452.

- Lechnerová, R., Helisová, K., and Benesš, V. (2008). Cox point processes driven by Ornstein-Uhlenbeck type processes. *Methodology and Computing in Applied Probability*, 10:315–335.
- Legg, M. W. and Chitre, M. A. (2012). Clustering of snapping shrimp snaps on long time scales: a simulation study. *Proceedings of Acoustics*.
- Møller, J., Syversveen, A. R., and Waagepetersen, R. P. (1998). Log Gaussian Cox processes. *Scandinavian Journal of Statistics*, 25:451–482.
- Øksendal, B. K. (1998). *Stochastic Differential Equations: An Introduction with Applications*. Berlin: Springer-Verlag.
- Papaspiliopoulos, O., Roberts, G. O., and Sköld, M. (2007). A general framework for the parametrization of hierarchical models. *Statistical Science*, 22:59–73.
- Roberts, G. and Sangalli, L. M. (2010). Latent diffusion models for survival analysis. *Bernoulli*, 16:435–458.
- Sermaidis, G., Papaspiliopoulos, O., Roberts, G. O., Beskos, A., and Fearnhead, P. (2012). Markov chain Monte Carlo for exact inference for diffusions. *Scandinavian Journal of Statistics*, 40:294–321.

# Appendix A - Auxiliary results

## A1. Sampling from a biased Brownian bridge

Suppose that the (normal) distribution of  $\tilde{X}$  under a  $BB(X_{\tau_1}, \tau_1, X_{\tau_2}, \tau_2)$  has mean vector  $\mu$  and covariance matrix  $\Sigma$ . Now define  $\mu_0$  to be a  $L$ -dimensional vector with all entries equal to  $b$ . Sampling from (7) can be performed via rejection sampling by proposing a value  $x$  from the distribution

$$\mathcal{N}(m, C), \quad C^{-1} = \Sigma^{-1}, \quad m = C(\Sigma^{-1}\mu + \mu_0), \quad (23)$$

and accepting with probability

$$\alpha = \prod_{l=1}^L \frac{g(x; \theta)}{\exp(bx + c)}. \quad (24)$$

If some additional conditions are satisfied though, more efficient algorithms can be used to simulate from (7). We present some examples below

- **Sampling from  $\tilde{\mathbb{W}}^*$  when  $g(u; \theta) \propto \exp\{-au^2 + bu\}$ , for  $a \geq 0, b \in \mathbb{R}$**

This implies that the density in (7) is a multivariate normal. Suppose first that  $a > 0$ , then the distribution of  $\tilde{X}$  under  $\tilde{\mathbb{W}}^*$  is

$$\mathcal{N}(m, C), \quad C^{-1} = \Sigma^{-1} + \Sigma_0, \quad m = C(\Sigma^{-1}\mu + \mu_0), \quad (25)$$

where  $\Sigma_0 = (2a)I_L$ , for  $I_L$  being the  $L$ -dimensional identity matrix.

If  $a = 0$ , the distribution of  $\tilde{X}$  under  $\tilde{\mathbb{W}}^*$  is given by (23).

- **Sampling from  $\tilde{\mathbb{W}}^*$  when  $g(u; \theta) \propto \Phi\{au + b\}$ , for  $(a, b) \in \mathbb{R}^2$**

This implies that the distribution of  $\tilde{X}$  belongs to a general class of skew-normal distributions from which directly simulation is not feasible. Two options are available here. The first is a rejection sampling that proposes from  $\mathcal{N}(\mu, \Sigma)$  and accepts with probability

$$\alpha = \prod_{l=1}^L \Phi(ax + b). \quad (26)$$

This algorithm has a global acceptance probability equals to  $\mathbb{E}[\prod_{l=1}^L \Phi(ax + b)]$ .

If the first algorithm is not efficient, simulation from (7) may be performed by considering an auxiliary embedded Gibbs sampling algorithm, as proposed by Gonçalves and Gamerman (2018). Define  $W = aI_L$  and  $\delta$  as the  $L$ -dimensional column vector with all entries equal to  $-b$ . Also define  $\Gamma = I_L + W\Sigma W'$ ,  $\Delta' = W\Sigma$  and  $\gamma = W\mu$ . Furthermore, let  $A$  be the lower diagonal matrix obtained from the Cholesky decomposition of  $\Gamma$ , i.e.  $\Gamma = AA'$ . Finally, define the region  $B = \{x \in \mathbb{R}^L; Ax > -(\gamma + \delta)\}$  and the  $L$ -dimensional random vectors  $U_0^*$ ,

$U_0$  and  $U_1$ . The following algorithm outputs an exact draw from (7).

1. Simulate  $(U_0^* | U_0^* \in B)$ , where  $U_0^* \sim \mathcal{N}(0, I_L)$ ;
2. obtain  $U_0 = AU_0^*$ ;
3. simulate  $(U_1 | U_0) \sim \mathcal{N}(\Delta\Gamma^{-1}U_0, \Sigma - \Delta\Gamma^{-1}\Delta')$ ;
4. output  $U_1 + \mu$ .

The only non-trivial step from the algorithm above is Step 1, in which we need to simulate from a vector of uncorrelated standard Gaussian distribution truncated to be in a region defined by linear constraints. That is achievable by a Gibbs sampler that samples each coordinate at a time from its respective univariate truncated standard normal full conditional distribution. The algorithm is efficient since the linear constraints are define by the lower diagonal matrix  $A$ , which allows us to initiate the algorithm already inside the truncated region  $B$ . Furthermore, the dimension  $L$  will typically be small, which makes the algorithm above sufficiently fast. More details about the simulation of this general class of skew normal distributions can be found in Gonçalves and Gamerman (2018).

- **Sampling from  $\tilde{\mathbb{W}}^*$  when  $g(u; \theta)$  is bounded by  $\exp\{-au^2 + bu + c\}$ ,  $\forall u \in \mathbb{R}$ , for  $a > 0$ ,  $(b, c) \in \mathbb{R}^2$**

We sample from (7) via rejection sampling by proposing a value  $x$  from (25) and accepting with probability

$$\alpha = \prod_{l=1}^L \frac{g(x; \theta)}{\exp(-ax^2 + bx + c)}. \quad (27)$$

- **Sampling from  $\tilde{\mathbb{W}}^*$  when  $g$  is uniformly bounded above by  $M$**

We sample from (7) via rejection sampling by proposing a value  $x$  from a  $\mathcal{N}(\mu, \Sigma)$  and accepting with probability

$$\alpha = \prod_{l=1}^L \frac{g(x; \theta)}{M}. \quad (28)$$

If direct simulation from (7) is not possible and more than one of the rejection sampling algorithms above can be applied, we choose the one with the highest global acceptance probability, which may be computed analytically or empirically.

## A2. The layered Brownian bridge

Define  $\phi(\cdot) = \left(g + \frac{\alpha^2 + \alpha'}{2}\right)(\cdot)$  and  $m(\theta) = \inf_{u \in \mathcal{X}} \{\phi(u; \theta)\}$ . Bounds for the  $\phi$  function are obtained from bounds on the Brownian bridge proposal which, in turn, are obtained through the *layered Brownian bridge* construction presented in Beskos et al. (2008). We ask the reader to resort to the original reference and Gonçalves et al. (2017) for details about the simulation of layers and of the process given layers. In fact, we perform the layer construction by simulating layers for standard (starting and ending

in 0) Brownian bridges on the respective time lengths and making the corresponding linear transformation to recover the layers for the original bridge (for details, see Gonçalves et al., 2017). This strategy produces tighter bounds for the diffusion path which in turn reduces the computational cost. Also, the parametrisation considered in Theorem 2 requires the simulation of standard bridges.

We define an upper bound  $r_{ij}(X)$  for function  $\phi$  in  $[s_{ij-1}, s_{ij}]$  as follows:

$$\phi_{i,lj}(\theta) = \inf \{ \phi(u; \theta); u \in B_{i,L,j} \}, \quad (29)$$

$$\phi_{i,u_j}(\theta) = \sup \{ \phi(u; \theta); u \in B_{i,L,j} \}, \quad (30)$$

$$r_{ij}(\theta) = \phi_{i,u_j}(\theta) - \phi_{i,lj}(\theta); u \in B_{i,L,j}, \quad (31)$$

where

$$B_{i,L,j} := [\underline{x}_{ij} + \underline{L}_{ij}, \bar{x}_{ij} + \bar{L}_{ij}], \quad j = 1, \dots, n_i + 1, \quad (32)$$

with  $\underline{x}_j = \min\{X_{s_{ij-1}}, X_{s_{ij}}\}$ ,  $\bar{x}_{ij} = \max\{X_{s_{ij-1}}, X_{s_{ij}}\}$ ,  $\underline{L}_{ij}$  and  $\bar{L}_{ij}$  being lower and upper bounds for the independent standard BB's in  $(s_{ij-1}, s_{ij})$ .

### A3. Sampling the partition $\tau$

The random partition  $\tau$  is updated on every iteration of the Gibbs sampler by setting a time length  $\varepsilon$  and doing as follows:

- i)  $\tau_1 \sim \mathcal{U}(0, \min\{\varepsilon, t_1\})$ ;
- ii)  $\tau_2 = \tau_1 + \varepsilon$ , if  $t_1 > \varepsilon$  and  $\tau_2 = \tau_1 + \mathcal{U}(0, \varepsilon)$ , otherwise;
- iii)  $\tau_j = \tau_1 + (l - 1)\varepsilon$ , for  $l = 3, \dots, m - 1$ ;
- iv)  $\tau_m = \tau_{m-1} + \varepsilon$ , if  $\tau_m \in (t_n, T)$  and  $t_m + \varepsilon > T$  for some  $m$ ; and  $\tau_m = \mathcal{U}(t_n, T)$ , otherwise.

### A4. Important results and definitions

We set, for  $i = 0, \dots, m$ ,

$$L(X, \theta) \propto \exp \left\{ - \int_0^T g(X_s; \theta) ds \right\} \prod_{j=1}^n g(X_{t_j}; \theta), \quad (33)$$

$$L_i(X, \theta) \propto \exp \left\{ - \int_{\tau_i}^{\tau_{i+1}} g(X_s; \theta) ds \right\} \prod_{j=1}^{n_i} g(X_{s_{ij}}; \theta), \quad (34)$$

$$\mathcal{G}(X, \theta) = \exp \left\{ - \int_0^T \left( \frac{\alpha^2 + \alpha'}{2} \right) (X_s; \theta) ds \right\}, \quad (35)$$

$$\mathcal{G}_i(X, \theta) = \exp \left\{ - \int_{\tau_i}^{\tau_{i+1}} \left( \frac{\alpha^2 + \alpha'}{2} \right) (X_s; \theta) ds \right\}. \quad (36)$$

$L(X, \theta)$  is the Poisson process likelihood, which is proportional to the RN derivative between the law of a  $PP(g(X_s; \theta))$  and the law of a  $PP(1)$ .  $\mathcal{G}_i(X, \theta)$  is proportional to the RN derivative between the law of a bridge of  $X$  in  $(\tau_i, \tau_{i+1})$  and the law of a Brownian bridge in the same interval and with same initial and end values (see Beskos et al., 2006b).

We now state the following results.

**Proposition 1.** *Let  $\tilde{\mathbb{P}}_i$ ,  $i = 0, \dots, m$ , be the probability measure of  $(\tilde{X}_i, \dot{X}_i | X_{\tau_i}, X_{\tau_{i+1}}, N, \theta, X_{-i})$ , where  $X_{-i}$  is  $X$  outside  $[\tau_i, \tau_{i+1}]$ . Then, the RN derivative of  $\tilde{\mathbb{P}}_i$  w.r.t. the law  $\tilde{\mathbb{W}}_i$  of a Brownian bridge is given by*

$$\frac{d\tilde{\mathbb{P}}_i}{d\tilde{\mathbb{W}}_i}(X) \propto L_i(X, \theta)\mathcal{G}_i(X, \theta), \quad (37)$$

**Proof.** See Appendix C.

**Proposition 2.** *Let  $\mathbb{P}_0$  be the probability measure of  $(X_0, \dot{X}_0 | N, X_{\tau_1}, \theta, X_{-0})$  and  $\mathbb{W}_0$  be the measure of a Brownian motion in  $[0, \tau_1)$  with initial distribution  $f_0$ , where  $X_{-0}$  is  $X$  outside  $[0, \tau_1]$ . Let also  $\mathbb{P}_m$  be the probability measure of  $(X_T, \dot{X}_m | N, X_{\tau_m}, \theta, X_{-m})$  and  $\mathbb{W}_m$  be the measure of a Brownian motion in  $(\tau_m, T]$ , where  $X_{-m}$  is  $X$  outside  $[\tau_m, T]$ . Then, the RN derivatives of  $\mathbb{P}_0$  w.r.t.  $\mathbb{W}_0$  and of  $\mathbb{P}_m$  w.r.t.  $\mathbb{W}_m$  are given by*

$$\frac{d\mathbb{P}_0}{d\mathbb{W}_0}(X) \propto L_0(X, \theta)\mathcal{G}_0(X, \theta) \exp\{-A(X_0; \theta)\} \quad (38)$$

$$\frac{d\mathbb{P}_m}{d\mathbb{W}_m}(X) \propto L_m(X, \theta)\mathcal{G}_m(X, \theta) \exp\{A(X_T; \theta)\} \quad (39)$$

**Proof.** See Appendix C.

**Lemma 1.** *The joint density of  $(\tilde{X}_i, \dot{X}_i, \mathcal{L}_i, \Xi_i | X_{\tau_i}, X_{\tau_{i+1}}, N, \theta)$ ,  $i = 0, \dots, m$ , with respect to the dominating measure  $\mathbb{L}^{n_i} \otimes \tilde{\mathbb{W}}_i \otimes \Xi_i^+$  is given by*

$$\begin{aligned} & \pi(\tilde{X}_i, \dot{X}_i, \mathcal{L}_i, \Xi_i | N, X_{\tau_i}, X_{\tau_{i+1}}, \theta, I_i = 1) = \pi(\tilde{X}_i, \dot{X}_i, \mathcal{L}_i^*, \Xi_i^* | N, X_{\tau_i}, X_{\tau_{i+1}}, \theta) \\ & = \pi_{\tilde{\mathbb{W}}_i^*}(\tilde{X}_i) \frac{\exp\left\{\sum_{j=1}^{n_i+1} \Delta_{ij}(1 - r_{ij}(\theta))\right\} \prod_{j=1}^{n_i+1} r_{ij}(\theta)^{\kappa_{ij}} \exp\left\{-\sum_{j=1}^{n_i+1} \Delta_{ij}((\phi_{i,lj} - m)(\theta))\right\}}{a_i(X_{\tau_i}, X_{\tau_{i+1}}; \theta)} \\ & \times \prod_{j=1}^{n_i+1} \prod_{l=1}^{\kappa_{ij}} \mathbb{I} \left[ \frac{\phi(\dot{X}_{\psi_{l,i,j}}; \theta) - \phi_{i,lj}(\theta)}{r_{ij}(\theta)} < v_{l,i,j} \right], \end{aligned} \quad (40)$$

where  $\pi_{\tilde{\mathbb{W}}_i^*}(\tilde{X}_i)$  is given by (7) for intervals with events from  $N$ , and is 1, otherwise. Also,

$$a(X_{\tau_i}, X_{\tau_{i+1}}; \theta) = \mathbb{E}_{\tilde{\mathbb{W}}_i^*} \left[ \exp \left\{ - \int_{\tau_i}^{\tau_{i+1}} \phi(X_s; \theta) - m(\theta) ds \right\} \right]. \quad (41)$$

**Proof.** See Appendix C.

## Appendix B - Simulated examples

Simulation from the model proposed in (2)-(5) is achieved by basically combining exact simulation of diffusions with the Poisson thinning technique that simulates a non-homogeneous Poisson process with intensity  $\lambda_s$  by thinning the events from a homogeneous Poisson process with intensity  $\lambda^*$  - an upper bound for  $\lambda_s$ ,  $\forall s$ . Exact simulation of diffusions is performed via the EA algorithm proposed in Beskos et al. (2006a) and Beskos et al. (2008). The EA algorithm samples from the exact law of a class of diffusion processes via retrospective rejection sampling. It proposes from (biased) Brownian motion in the case of unconditional diffusions and from Brownian bridge in the case of diffusion bridges. The algorithm is directly applied to unit diffusion coefficient processes which can always be obtained, if  $\sigma$  is differentiable, by applying the Lamperti transform. The acceptance probability of EA has the form  $\exp\left\{-\int_0^t \phi(X_s)ds\right\}$ , where  $\phi(x) = \left(\frac{\alpha^2 + \alpha'}{2}\right)(x) - l$  and  $l = \inf_{u \in \mathbb{R}} (\alpha^2 + \alpha')(u)/2$ . The decision whether or not to accept the proposal is taken by means of a Poisson process in such a way that the path of  $X$  only needs to be unveiled at a random finite collection of time points.

Suppose, without loss of generality, that the simulation of  $X$  requires the simulation of layers (see Appendix A2) for the Brownian bridge proposal and function  $g$  in (3) is unbounded. The algorithm to simulate DDCP's is as follows:

### Exact simulation of DDCP's

1. simulate  $X_0$  from  $f_0$ ;
2. simulate  $X$  in  $(0, t]$  via EA and keep the lower and upper bounds for  $X$  obtained from the layers;
3. obtain an upper bound  $\lambda^*$  for  $\lambda_s$  in  $[0, t]$  using the bounds for  $X$ ;
4. simulate a Poisson process of rate  $\lambda^*$  on  $[0, t]$ :  $(t_1, \dots, t_{n^*})$ ;
5. simulate  $X$  at times  $(t_1, \dots, t_{n^*})$ , from the respective layered BB;
6. keep each of the  $n^*$  points with probability  $R(t_i) = \frac{\lambda(t_i)}{\lambda^*}$ .

Step 2 should be performed piecewise if  $t$  is big, in order to get a reasonable computational cost (see Beskos et al., 2006a). In this case, each simulated interval provides an upper bound  $\lambda^*$  based on its layers.

We simulate four Cox processes. For the OU-process  $dX_s = \rho X_s ds + dW_s$ , we consider  $g(X_s) = \exp(\mu + \sigma X_s)$  (exp-OU), for  $\mu = 0$ ,  $\rho = 0.05$ ,  $\sigma = 0.2$ ; and  $g(X_s) = \delta \Phi(\sigma X_s)$  (cdf-OU), for  $\rho = 0.05$ ,  $\sigma = 0.2$ ,  $\delta = 3$ . For the (transformed) DW process  $dX_s = -\rho X_s(\sigma^2 X_s^2 - \mu)ds + dW_s$ ,  $g(X_s) = \exp(\delta + \sigma X_s)$  (exp-DW), for  $\delta = 0$ ,  $\mu = 1.5$ ,  $\rho = 0.05$ ,  $\sigma = 0.15$ ; and  $g(X_s) = \delta \Phi(\sigma X_s)$  (cdf-DW), for  $\mu = 0.5$ ,  $\rho = 0.1$ ,  $\sigma = 0.2$ ,  $\delta = 3$ .

Figure 6 shows one realisation of each of the four processes, with  $T = 400$ . We also compute Monte Carlo estimates of the expectation of some functionals of the processes, which are presented in Table 4.



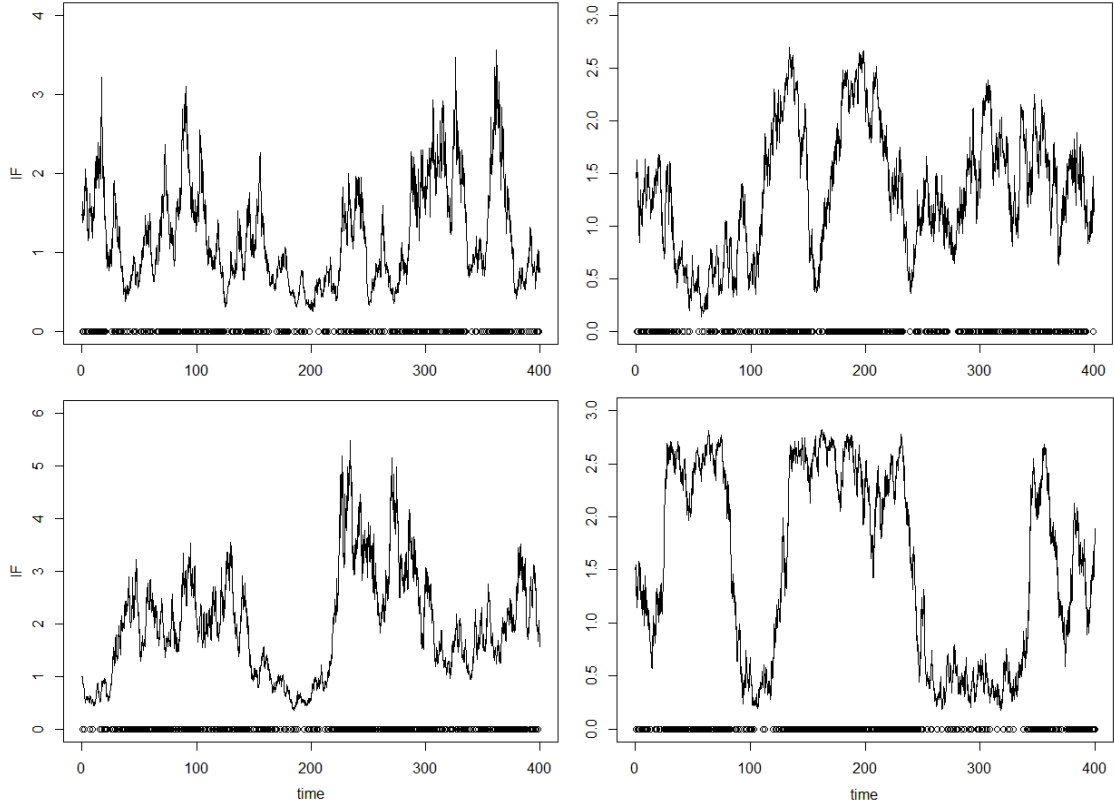


Figure 6: Realisation of processes exp-OU (top-left), cdf-OU (top-right), exp-DW (bottom-left) and cdf-DW (bottom-right). Number of Poisson events are 499, 518, 714 and 645, respectively.

		1%	25%	50%	75%	99%	mean	s.d.
exp-OU	$N_T$	294	415	477	549	773	487.34	102.74
	$t_{(10)}$	1.83	5.91	9.32	14.24	34.01	10.95	6.93
cdf-OU	$N_T$	410	543	599	656	792	599.58	82.90
	$t_{(10)}$	2.14	4.64	6.61	9.84	28.06	8.10	5.31
exp-DW	$N_T$	118	167	654	1171	1408	681.20	469.68
	$t_{(10)}$	3.70	7.08	9.40	13.30	38.12	11.43	6.89
cdf-DW	$N_T$	144	218	602	976	1084	601.20	349.69
	$t_{(10)}$	2.66	5.05	6.50	8.55	25.40	7.49	4.19

Table 4: Monte Carlo estimates of the expectation of some functionals of the simulated processes. An iid sample of size 50k is used.  $N_T$  is the number of Poisson events,  $t_{(10)}$  is the time of occurrence of the 10-th event.

## Appendix C - proofs

### Proof of Proposition 1

Bayes Theorem gives

$$\begin{aligned}
\frac{d\tilde{\mathbb{P}}_i}{d\tilde{\mathbb{W}}_i}(\tilde{X}_i, \dot{X}_i) &\propto \frac{dP}{dN}(N|\cdot) \frac{d\tilde{\mathbb{P}}_i}{d\tilde{\mathbb{W}}_i}(\tilde{X}_i, \dot{X}_i | X_{\tau_{i+1}}, X_{\tau_i}, \theta) \\
&\propto \frac{dP}{dN}(N|\cdot) \frac{d\tilde{\mathbb{P}}_i}{d\tilde{\mathbb{W}}_i}(\tilde{X}_i, \dot{X}_i, X_{\tau_{i+1}} | X_{\tau_i}, \theta) \frac{\pi_{\tilde{\mathbb{W}}_i}(X_{\tau_{i+1}} | X_{\tau_i}, \theta)}{\pi_{\tilde{\mathbb{P}}_i}} \propto L_i(X, \theta) \mathcal{G}_i,
\end{aligned}$$

where  $\mathcal{G}_i$  is obtained from Girsanov's Theorem (see Beskos et al., 2006a, Equation (4)).  $\square$

## Proof of Proposition 2

From Bayes Theorem

$$\begin{aligned}
\frac{d\mathbb{P}_0}{d\mathbb{W}_0}(X) &\propto \frac{d\mathbb{P}}{dN}(N|\cdot) \frac{d\mathbb{P}_0}{d\mathbb{W}_0}(X_0, \dot{X}_0 | X_{\tau_1}, \theta) \\
&\propto L_0(X, \theta) \frac{d\mathbb{P}_0}{d\mathbb{W}_0}(\dot{X}_0, X_{\tau_1} | X_0, \theta) \frac{f_0}{f_0}(X_0; \theta) \\
&\propto L_0(X, \theta) \mathcal{G}_0 \exp \{-A(X_0; \theta)\}.
\end{aligned}$$

Analogously,

$$\begin{aligned}
\frac{d\mathbb{P}_m}{d\mathbb{W}_m}(X) &\propto \frac{d\mathbb{P}}{dN}(N|\cdot) \frac{d\mathbb{P}_m}{d\mathbb{W}_m}(X_T, \dot{X}_m | X_{\tau_m}, \theta) \\
&\propto L_m(X, \theta) \mathcal{G}_m \exp \{-A(X_T; \theta)\},
\end{aligned}$$

where  $\mathcal{G}_1$  and  $\mathcal{G}_m$  are obtained from Girsanov's Theorem (see Beskos et al., 2006a, Equation (4)).  $\square$

## Proof of Lemma 1

The result is proved by showing that the output from a rejection sampling algorithm that proposes  $(\tilde{X}_i, \dot{X}_i, \mathcal{L}_i)$  from  $\tilde{\mathbb{W}}_i^*$  and  $\Xi_i$  from its marginal law and has acceptance indicator given by (20) is an exact draw from  $(\tilde{X}_i, \dot{X}_i, \mathcal{L}_i, \Xi_i | X_{\tau_i}, X_{\tau_{i+1}}, N, \theta)$ .

Let  $\tilde{\mathbb{P}}_i$  be the law of  $(\tilde{X}_i, \dot{X}_i, \mathcal{L}_i | X_{\tau_i}, X_{\tau_{i+1}}, N, \theta)$ , then, equation (34) and Proposition 1 imply that

$$\frac{d\tilde{\mathbb{P}}_i}{d\tilde{\mathbb{W}}_i^*}(X) = \frac{d\tilde{\mathbb{P}}_i}{d\tilde{\mathbb{W}}_i}(X) \frac{d\tilde{\mathbb{W}}_i}{d\tilde{\mathbb{W}}_i^*}(X) \propto \exp \left\{ - \int_{\tau_i}^{\tau_{i+1}} \phi(X_s; \theta) - m(\theta) ds \right\} \leq 1. \quad (42)$$

The proof is concluded by noticing that

$$\begin{aligned}
&\exp \left\{ - \int_{\tau_i}^{\tau_{i+1}} \phi(X_s; \theta) - m(\theta) ds \right\} = \\
&\prod_{j=1}^{n_i+1} \exp \left( -(s_{ij} - s_{ij-1})(\phi_{lj}(\theta) - m(\theta)) - \int_{s_{ij-1}}^{s_{ij}} \phi(X_s; \theta) - \phi_{lj}(\theta) ds \right),
\end{aligned}$$

and noticing that this is equal to  $P(I_i = 1)$ .

□

## Proof of Theorem 1

We have that

$$\begin{aligned} & \pi(N, \mathcal{L}, \tilde{X}, \dot{X}, \Xi, X_0, \theta) \propto \\ & \prod_{i=0}^m \pi(\tilde{X}_i, \dot{X}_i, \mathcal{L}_i, \Xi_i | X_{\tau_i}, X_{\tau_{i+1}}, N, \theta) \pi(X_\tau, N | X_0, \theta) \pi(X_0 | \theta) \pi(\theta). \end{aligned} \quad (43)$$

The first term on the right-hand side of (43) is obtained from Lemma 1. To derive the second term we define  $\mathbb{P}$  and  $\tilde{\mathbb{P}}$  to be the probability measures of  $(X_{-\tau}, X_\tau, N | \theta)$  and  $(X_{-\tau} | X_\tau, N, \theta)$ , respectively, where  $X_{-\tau} := X \setminus X_\tau$ . We also define  $\tilde{\mathbb{W}}^*$  to be the joint measure of the  $m + 1$  biased Brownian bridges  $BB(\tau_i, X_{\tau_i}; \tau_{i+1}, X_{\tau_{i+1}})$ , for  $i = 1, \dots, m + 1$ , as defined in Appendix A1.

We now obtain the joint density  $\pi(X_\tau, N | X_0, \theta)$  w.r.t. the product measure  $(\mathbb{N} \otimes \mathbb{L}^{m+1})$ . We have that

$$\frac{d\tilde{\mathbb{P}}}{d\tilde{\mathbb{W}}^*}(X) = \frac{d\tilde{\mathbb{P}}}{d\tilde{\mathbb{W}}}(X) \frac{d\tilde{\mathbb{W}}}{d\tilde{\mathbb{W}}^*}(X), \quad (44)$$

and

$$\frac{d\tilde{\mathbb{W}}}{d\tilde{\mathbb{W}}^*}(X) = \frac{\pi_{\tilde{\mathbb{W}}}(\tilde{X})}{\frac{1}{c(\theta)} \pi_{\tilde{\mathbb{W}}}(\tilde{X}) \prod_{j=1}^n g(X_{t_j}; \theta)} = \frac{c(\theta)}{\prod_{j=1}^n g(X_{t_j}; \theta)}, \quad (45)$$

where  $c(\theta) = \prod_{i=1}^{m-1} c_i(\theta)$ .

Furthermore, Bayes theorem combined with ideas from Lemma 1 gives

$$\frac{d\tilde{\mathbb{P}}}{d\tilde{\mathbb{W}}}(X_{-\tau}) = L(X, \theta) \mathcal{G}(X, \theta) \exp \{A(X_T; \theta) - A(X_0; \theta)\} \frac{\prod_{i=0}^m f_{\mathcal{N}}(X_{\tau_{i+1}}; X_{\tau_i}, \Delta_i)}{\pi(X_\tau, X_T, N | X_0, \theta)}, \quad (46)$$

for  $L$  and  $\mathcal{G}$  as defined in (33) and (35), respectively.

If we replace (46) and (45) in (44) and take expectation on both sides w.r.t.  $\tilde{\mathbb{W}}^*$ , we get

$$\begin{aligned} \pi(X_\tau, N | X_0, \theta) &= \mathbb{E}_{\tilde{\mathbb{W}}^*} \left[ L(X, \theta) \mathcal{G}(X, \theta) \exp \{A(X_T; \theta) - A(X_0; \theta)\} \frac{1}{\prod_{j=1}^n g(X_{t_j}; \theta)} \right] \\ &= c(\theta) \prod_{i=0}^m f_{\mathcal{N}}(X_{\tau_{i+1}}; X_{\tau_i}, \Delta_i). \end{aligned} \quad (47)$$

We now replace (40) and (47) in (43) to get the result.

□

## Proof of Theorem 2

This is analogous to the proof of Theorem 1, but replacing  $(X_\tau, \tilde{X}, \dot{X})$  by  $(Y_\tau, \tilde{Y}, \dot{w})$ , where  $\dot{w}$  is a linear transformation  $\varphi^{-1}$  of the bridges among the  $(X_\tau, \tilde{X})$  values to make them start and end in 0. We get that

$$\pi(N, \mathcal{L}, \tilde{Y}, \dot{w}, \Xi, Y_0, \theta) \propto \prod_{i=0}^m \pi(\tilde{Y}_i, \dot{Y}_i, \mathcal{L}_i, \Xi_i | Y_{\tau_i}, Y_{\tau_{i+1}}, N, \theta) \pi(X_\tau(\theta), N | X_0(\theta), \theta) \prod_{i=0}^m \eta'(Y_{\tau_{i+1}}; \theta) \pi(Y_0 | \theta) \pi(\theta).$$

The first term on the right-hand side of (48) is obtained by adapting Lemma 1. Basically, by replacing  $\pi_{\tilde{W}_i}(\tilde{X}_i)$  with  $\pi_{\tilde{W}_i}(\tilde{X}_i(\theta); X_{\tau_i}(\theta), X_{\tau_{i+1}}(\theta)) \prod_{j=1}^{n_i} \eta'(Y_{s_{ij}}; \theta)$ , and redefining  $\phi_l$ ,  $\phi_u$  and  $m(\theta)$  as shown in the theorem. Furthermore, the Brownian bridges measure in the dominating measure is replaced by the measure of standard Brownian bridges (starting and ending in 0).

□

## Appendix D - MCMC plots

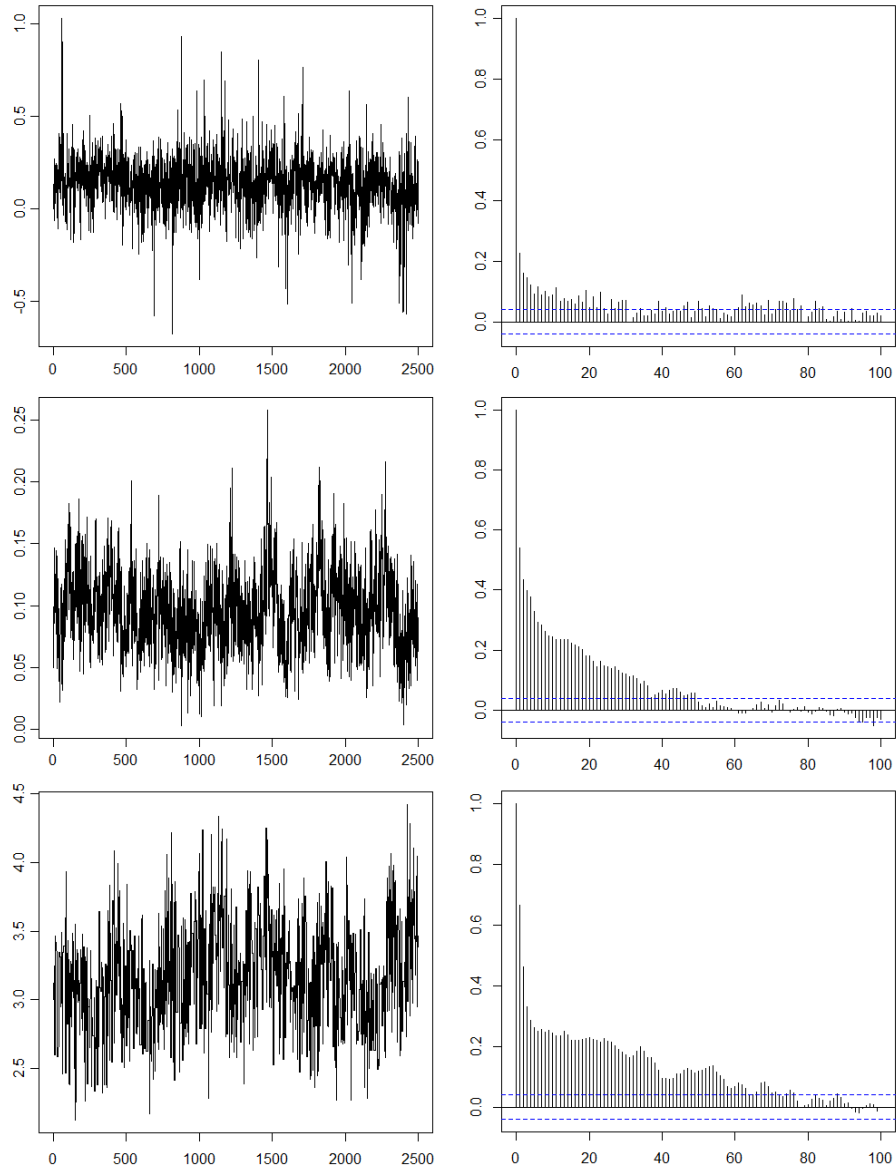


Figure 7: Trace plot and autocorrelation plot for the estimated parameters in the exp-OU and cdf-DW simulated example. Top:  $\mu$ , middle:  $\rho$ , bottom:  $\delta$ .

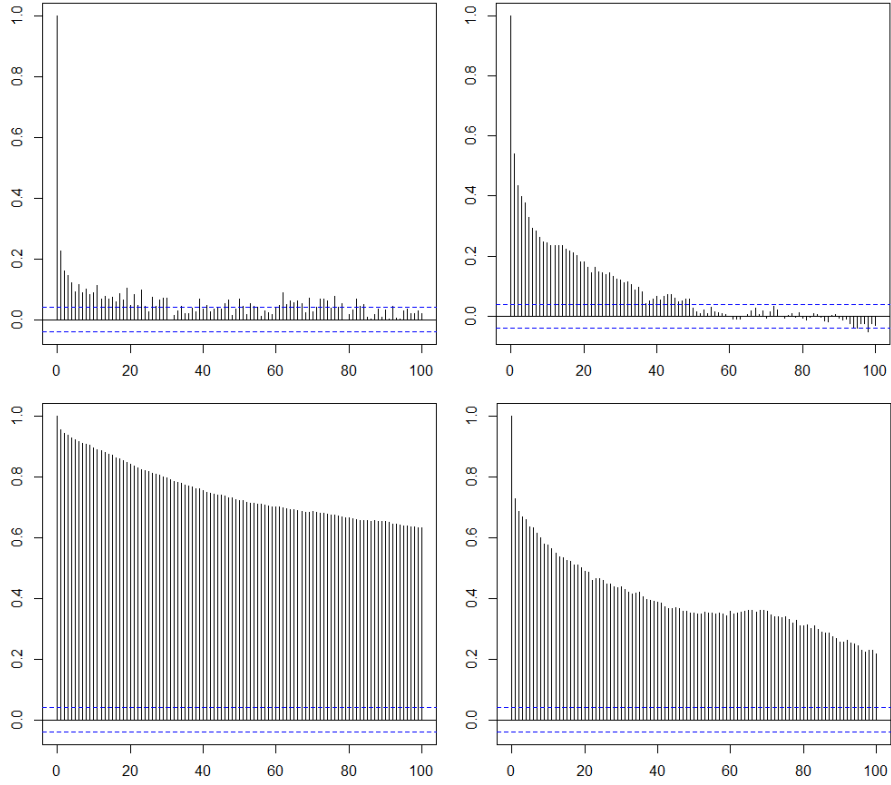


Figure 8: Autocorrelation plots of  $\mu$  (left) and  $\rho$  (right) for the exp-OU example under the centred (top) and noncentred (bottom) parametrisation.

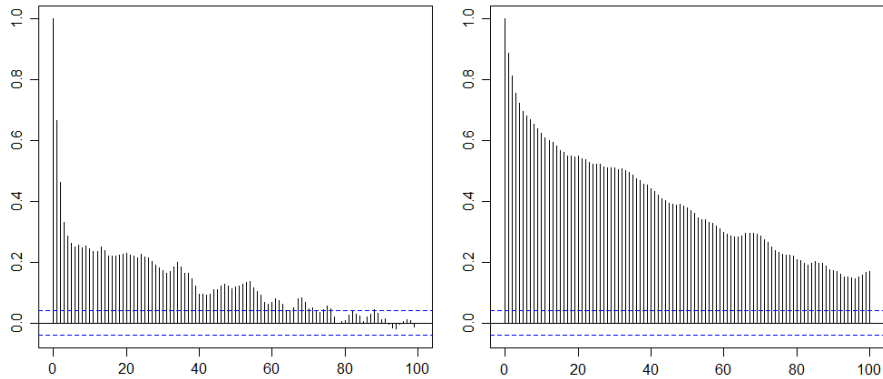


Figure 9: Autocorrelation plot of parameter  $\delta$  for the cdf-DW example under the noncentred (left) and centred (right) parametrisation of the Poisson processes  $\Xi_i$ .